Absolute Gain Determination of the AGIPD Detector

DESY Summer Students Program 2019

Bc. Slávka Martinková, University of Pavol Jozef Šafárik, Slovakia

Supervisor: Dr. Patrik Vagovič

EuXFEL, SPB Group

5.9.2019, Hamburg

Abstract

Successful scattering experiments at X-ray photon sources rely on prior characterisation and calibration of detectors involved. For the scattering experiments at European XFEL at SPB/SFX instrument major direct conversion detector used is AGIPD operating at 4.5 MHz sampling rate. To perform quantitative data analysis, the first important task is the calibration of the gain to understand the relation between ADU (Analog to Digital Unit) and number of photons detected. The goal of this summer project is to obtain basic knowledge for AGIPD data handling and perform the calibration. This work is focusing on a task of detector calibration. In the introduction AGIPD detector structure and design is briefly discussed. Next, the effects influencing the detector output signal are introduced, together with an approach of handily these effects. At the end, review of a gain determination procedure is shown. The aim is determinate relative gain of detector and bad pixel mask for modules of detector. This work is important for beginners who want to used detectors, such as AGIPD, for their experiments and further analysis.

Contents

1 Introduction

The European X-ray Free Electron Laser Facility (EuXFEL) produces extremely intensive, highly coherent, ultra-short X-ray pulses with a peak brilliance of $5x10^{33}$ *ph/ (s mm^2 mrad^2 0.1%BW)* in the energy range *0.25 keV – 25 keV* depending on the experimental station. X-ray pulses are delivered in bunch es (so called trains) with a repetition rate of *10 Hz*. Every train consists of up to *2700* pulses with approximately *10^{12}* photons. Between every pulses is time interval 220 ns. For example, when we take into account, that maximal pulses amount is *2700*, which are deliver during *600 ms*, pulse frequency is *4.5 MHz*. [7] These unique characteristics of the XFEL beam provide big potential for usage in various scientific areas, for example physics, chemistry, material engineering and biology. The properties of the EuXFEL beam put demanding requirements au X-ray imaging detectors, like e.g. match the time structure recording at *4.5 MHz*, high dynamic range, provide high level of radiation hardness. [8] One of the detectors meeting the above stated requirements is the AGIPD detector.

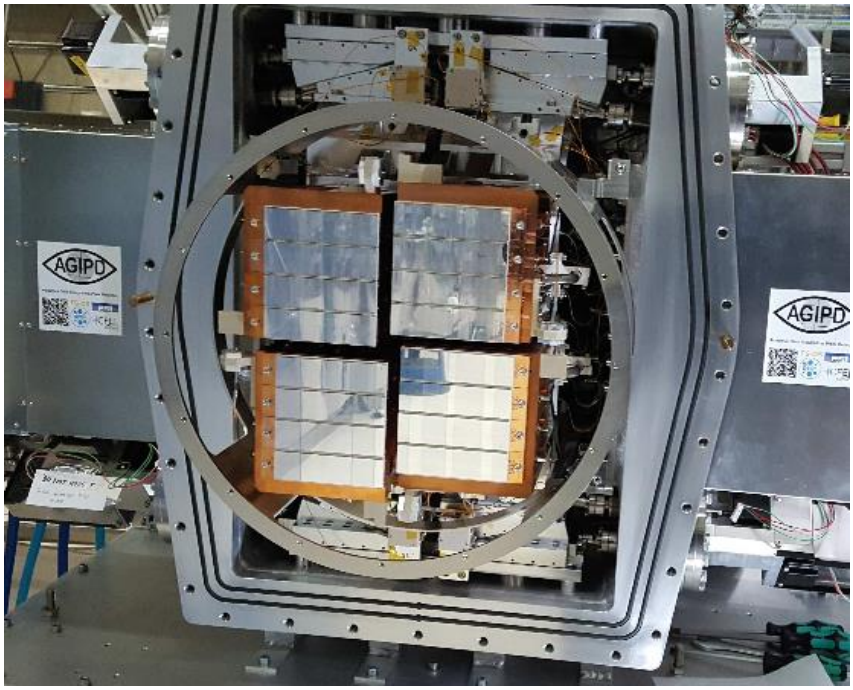

Figure 1. *Image of the AGIPD detector [1].*

2 AGIPD

2.1 Detector Structure

Adaptive Gain Integrating Pixel Detector (AGIPD) is a fast, hybrid pixel detector, consisting of 16 modules, where each module represents single detector system, as shown in Figure 1. Each module consists of four base parts: digital part, analogue part, vacuum board and detector head, as shown in Figure 2. X-rays are detected in detector head, by silicon sensor. The detected signal is digitalized by set of Application Specific Integrated Circuits (ASICs). The sensitive area comprises of *512x128* pixels, with a pixel size of *200x200* μm^2. Every module is connected with vacuum board, which provides a connection to ADC board, for analogue signal transmission and provides required power of ASIC circuits and sensors. Analogue part consists of *64* ADC canals in a two-board system. Analogue signal is digitalized with a *14-bit* resolution and then transferred to the digital part with a FPGA daughter card, which is used to process digital data. Processing of an analogue signal is implemented on each pixel to save 352 pictures recorded during the pulse burst lasting *0.6 ms*.

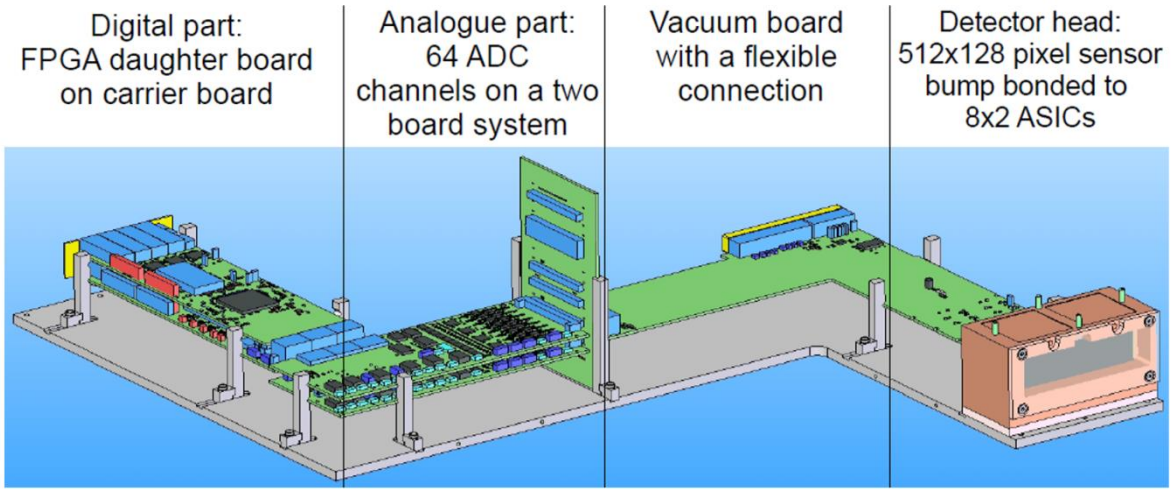

Figure 2. *Structure of the AGIPD single module [2].*

2.2 Mechanical Design

Mechanical construction of the AGIPD was designed to provide independent movement of all four quadrants. Movement of quadrants, as shown in Figure 3, is realized by motors fixed

to ramp blocks, which can be shifted, to allow opening and closing of a central aperture. Synchronized movement of quadrants in a horizontal and a vertical direction is also possible.

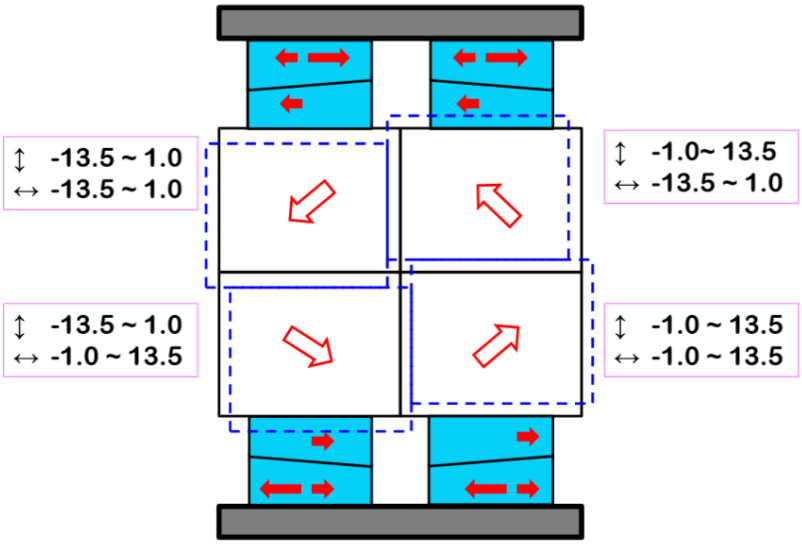

Figure 3. *Concept of an independent movement of all four detector quadrants. All numbers are in millimeters [3].*

Figure 4 shows construction of a hybrid system with eight motors for quadrants movement, installed outside the vacuum for lighter maintenance and easier heat dissipation. Module systems is installed on copper blocks, which are active cooling with external cooling device. Thanks to motors, the central aperture can be set to the maximum value *27x27 mm*^{2}.

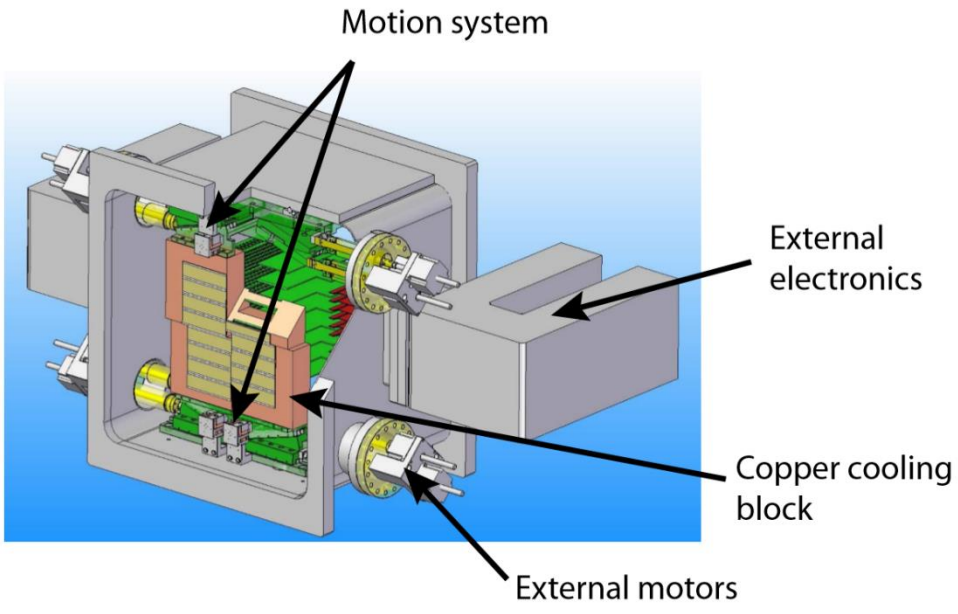

Figure 4. *Technical design of the AGIPD [3].*

3 Dark Signal of Detector

In order to produce scientific-quality of experimental data from the AGIPD detector the device needs to be properly calibrated. This part is focusing on the effects influencing the detector output signal are introduced, together with an approach of handily these effects.

3.1 Offset

The dark signal is a detector signal, measured without presence of an outside stimulus, for example incident photons. The dark signal $O_{i,j,m,g}$ is determined of a sum of two contributors, average value of dark current and a pedestal value of a detector,

$$O_{i,j,m,g} = \langle I_{Dark} \rangle + C_{offset}$$

where indexes *i, j* appertains to pixel coordinates and *m, g* to the memory-cell and gain-stage, where applicable. C_{offset} is a constant value of a detector pedestal both temperature and time independent. This value is added as a baseline to the system, in order to ease signal digitization. During data analysis, it is important to subtract the offset value from illuminated data. The dark current I_{Dark} is a nonzero part of signal, resulting from thermally generated electrons and leakage current.

3.2 Noise

Noise of detector includes many random factors, which introduce various uncertainties into the data. Therefore, it is very difficult to correctly determine it. Characterization of a detector noise is necessary, to quantify energy resolution of a detector or the uncertainties for photon integrating detectors. Commonly, it is determined as standard deviation of a dark signal. During correction of signal with electronic components, such as capacitive elements or amplifiers. The input signal accumulates additional noise. First type of noise is *Thermal noise*, created by fluctuations of the electron distribution in a semiconductor, leading to small noise voltage being induced between the two ends of a conductor with resistance *R*. Next type is *Low-frequency voltage noise*, its occurrence is typical for electronic devises, which are working on direct current. It created either due to changed resistance, which will the effect due to the Ohm´s

law, like changing of resistance or current, or from charges trapped in the semiconductor material, which induce currents in field effect transistors. The essence of another type of noise is in a discrete behavior of charge so called *Shot noise*. Last important noise type, which has to be taken into account is *Fano noise*. This is due to a fluctuation of electron-hole pairs generated from an X-ray of a given energy E in a semiconductor material.

In practice, for completely assembled detector is a study of single noise components is very demanding and lengthy. Therefore, total noise of a detector is determined as a standard deviation of all these noise components.

3.3 Bad Pixels

Bad pixels are pixels, which show higher values of noise comparing to average value or do not provide any signal. This can be caused by different physical or electronic effects. It is very important to identify these bad pixels and then remove them from data analysis, to maintain reliability and correct ness of data. To identify bad pixels, four filters implemented as thresholds are used. First two types of filters use threshold values against per-pixel offset $O_{i,j,m,g}$. Bad pixels exceeding upper threshold t_{hot} of offset are known as *hot pixels*, where: $O_{i,j,m,g} > t_{hot}$. Pixels with signal smaller than lower offset threshold t_{cold} are known as *cold pixels*, where: $O_{i,j,m,g} < t_{cold}$. The next two types of filters use threshold values against per-pixel noise $\sigma_{Dark,i,j,m,g}$. Bad pixels with a noise higher than the noise upper threshold t_{noisy} are known as *noisy pixels*, where: $\sigma_{Dark,i,j,m,g} > t_{noisy}$. Last type are *dead pixels*, they noise is smaller than the noise lower threshold t_{dead}, where: $\sigma_{Dark,i,j,m,g} < t_{dead}$.

4 Detector Data Analysis

For a detector characterization purposes, commonly, two sets of data are used: dark data (no incoming photons) and flat-field data (uniformly irradiated by photons). In first step it is necessary to subtract offset from flat-field data. Figure 5 shows single module of a detector before (left) and after (right) removing the offset. The AGIPD detector can work in different modes of data recording. In our case data was recorded gradually into the memory cells four pulses per train.

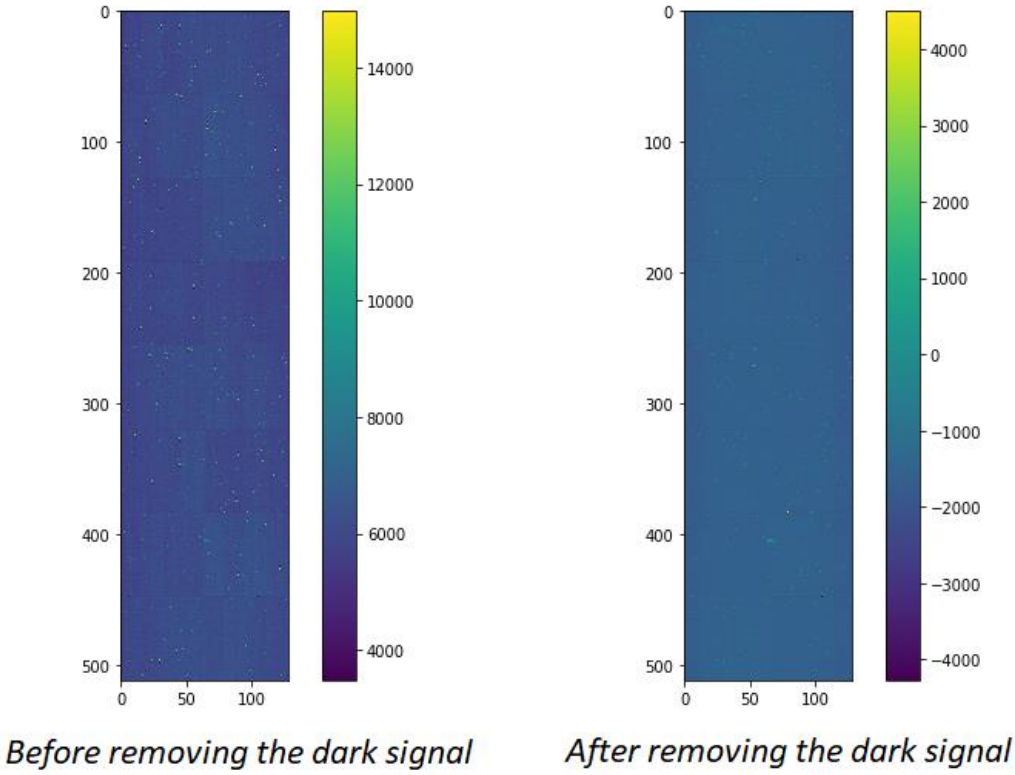

Figure 5. *Comparison of signal, before and after subtracting the offset, signal is in ADU (Analog-to-Digital Units)*

4.1 Absolute Gain of the AGIPD Detector

In the first step it is necessary to determinate dependence of ADU on changing train for a single memory cell of a single pixel illuminated with characteristic X-rays, which energy of single photon is *9.3 keV*. Figure 6 shows histogram of this dependence. First peak corresponds to background of the detector and the second two peaks to the multiples of single photons. Using peak-to-peak analysis we determine value ADU of individual multiples of single photons. Figure 7 shows this dependence. Subsequently fitting linear function to this dependency, the slope of linear function will represent the absolute gain of the detector: *7,66 ADU/keV*. This value determines the conversion factor between digital units *ADU* and energy units (*keV*).

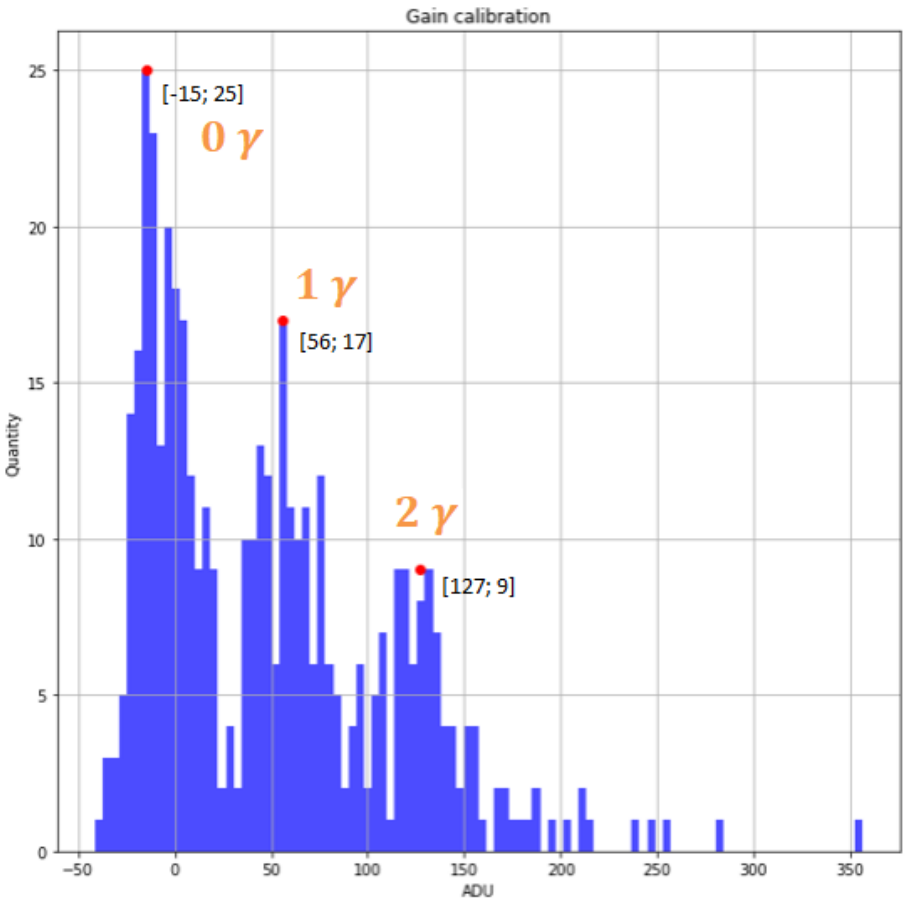

Figure 6. *Histogram of gain calibration*

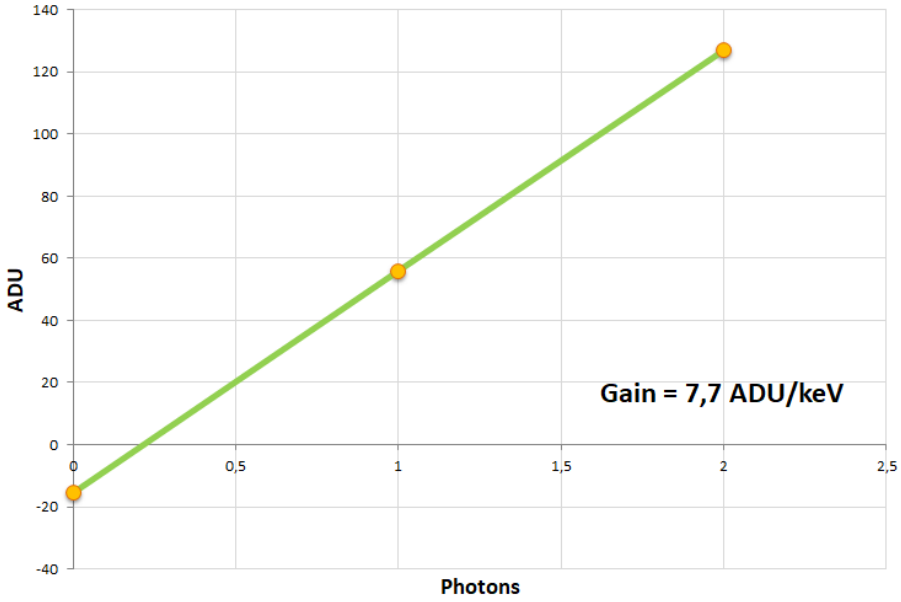

Figure 7. *Relative gain of detector*

4.2 Mask of bad pixels

Figure 8 shows photon spectrum for four memory cells, together with corresponding image of signal from module. It is to note, that first memory cell does not show any photon signal, output shows only noise. While signal from another memory cells is characterized with three peaks, the first peak corresponds to noise of the detector and second peaks to multiples of single photon.

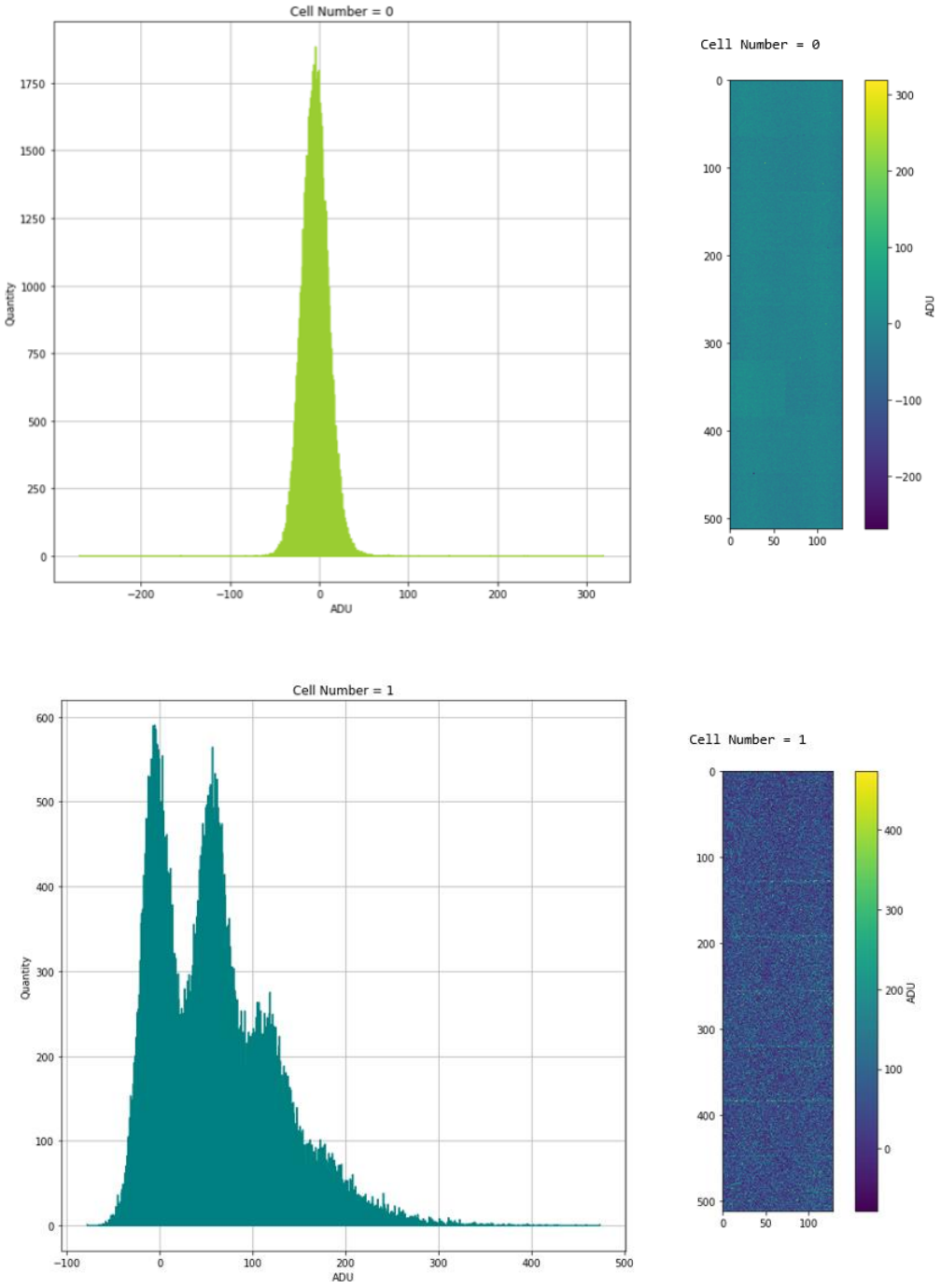

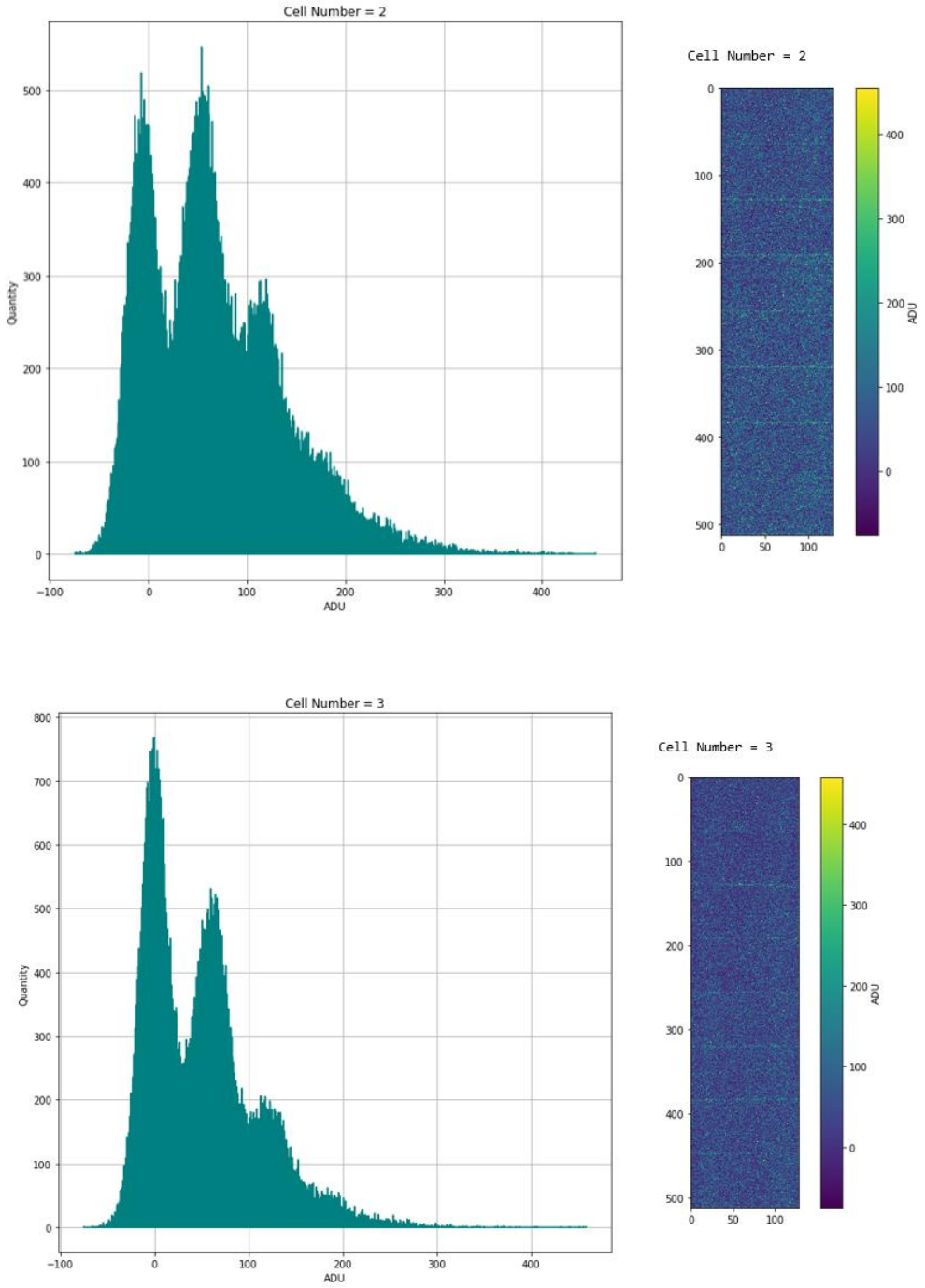

Figure 8. *On the left, photon spectrum for four memory cells and on the right, corresponding image of signal from module.*

Second step is to determinate standard deviation of the signal for a single memory cell, of a single pixel per train. Then determine how these standard deviations change in single module. Figure 9 shows distribution of standard deviations in pixel. This way we behavior individual pixels in memory cell can be observed. It can be seen that some pixels exhibit either

high or vice versa very low value. These can be defined as bad pixels, which needs to be removed.

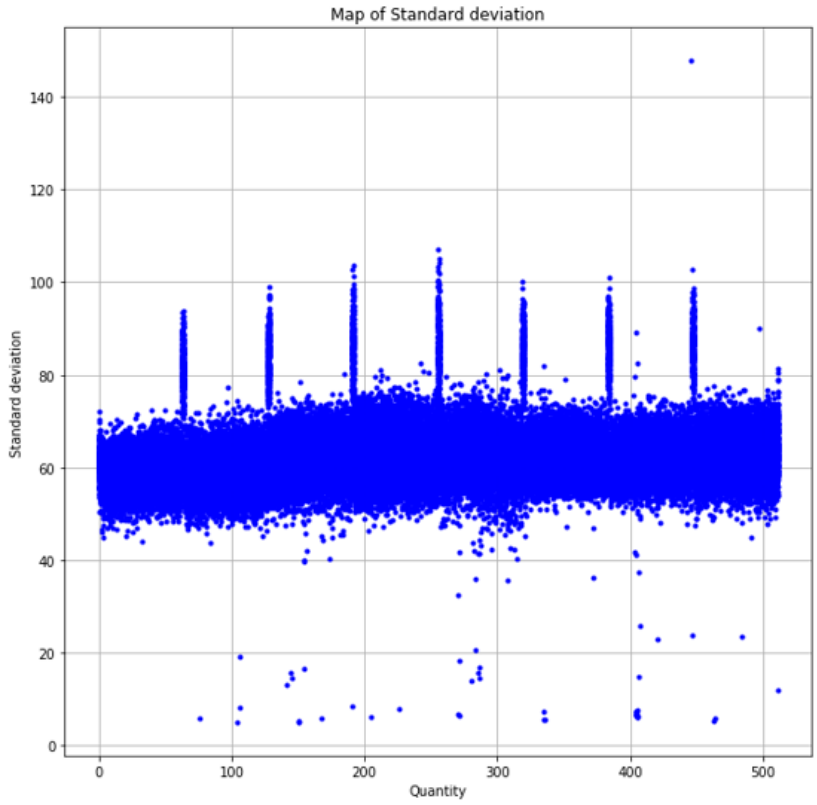

Figure 9. *Map of standard deviation*

Then the average value of standard deviation values can be determined. Thanks to the average thresholds to create a mask of bad pixels can be set. This mask can be applied to our data and so cause bad pixels removed from experimental data. Figure 10 shows map of standard deviation and a mask of bad pixels for two separate memory cells of the detector.

Figure 11 shows series of standard deviation maps and masks of bad pixels for several separate modules for one memory cell of the detector.

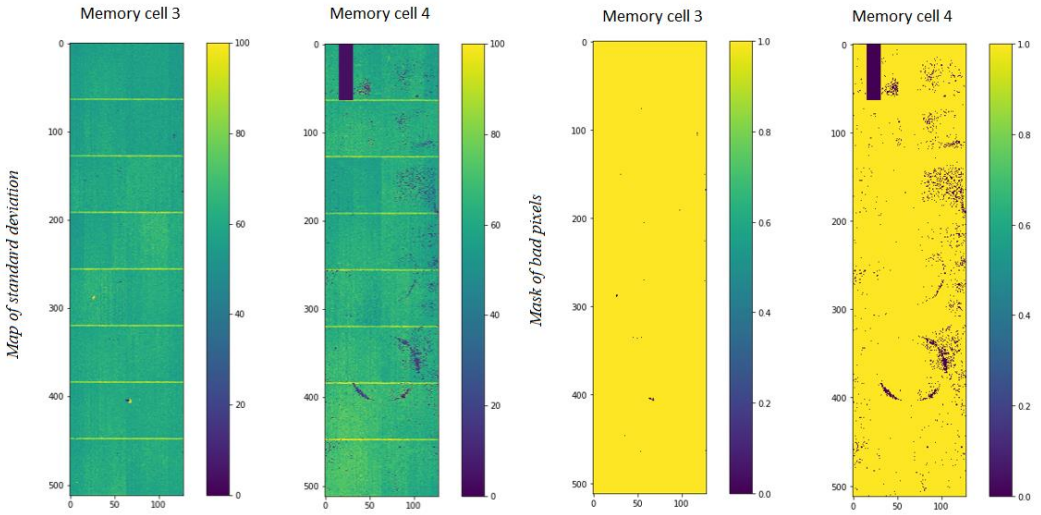

Figure 10. *On the left, maps of standard deviation and on the right, mask of bad pixels for two separate memory cells in one module of the detector.*

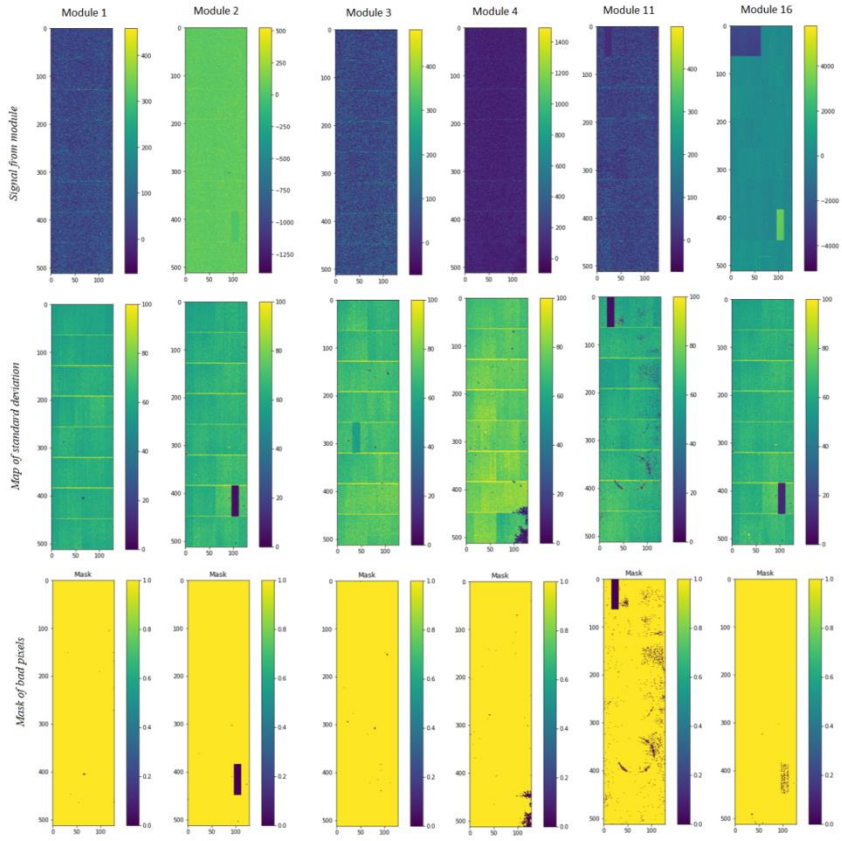

Figure 11. *Maps of standard deviation and masks of bad pixels for several separate modules for one memory cell of the detector.*

Conclusion

The goal of this summer project was to obtain basic knowledge for AGIPD data handling using python-based software tools with the focus to perform the absolute gain calibration. Two important tasks related to the detector characterization has been addressed and successfully solved. First task was to determine detector gain, which was determined to be *7.66 ADU/keV*. The detector gain is conversion constant between digital units (*ADU*) and energy units (*keV*). Second task was to identify bad pixels using statistical methods and generate mask which can be used for further data analysis. Using statistical analysis (described above) the bad pixels (dead pixels and noisy pixels) has been identified and the mask was generated.

Acknowledgements

I would like to express my thanks to *Ing. Karel Saksl DrSc.*, *Prof. Dr. Serguei Molodtsov*, *Dr. Adrian Mancuso* and my supervisor *Dr. Patrik Vagovic* for great opportunity to be involved in Summer School. Also, I would like to thank to *Dr. Patrik Vagovic* and *Mgr. Ivana Klačková* for their guidance and help at work throughout. Many thanks to *the XFEL SPB group*, for ensuring a feeling of welcome and camaraderie throughout the development of this project. Special thanks go es to *the DESY Summer Student Program organizers*, for arranging such an enjoyable and educational experience.

References

[1] https://www.xfel.eu/sites/sites_custom/site_xfel/content/e35152/e35161/e59605/e59607/e59608/e59616/xfel_file59619/Mancuso_XFEL_and_SPBSFX_for_Microfluidics_Workshop_eng.pdf

[2] A. Allahgholi, J. Becker, L. Bianco, A. Delfs, R. Dinapoli, P. Goettlicher, H. Graafsmaa, D. Greiffenberg, H. Hirsemann, S. Jacka R. Klanner, A. Klyuev, H. Krueger, S. Lange, A. Marras, D. Mezza, A. Mozzanica, S. Rah, Q. Xia, B. Schmitt, J. Schwandt, I. Sheviakov, X. Shi, S. Smoljanin, U. Trunk, J. Zhang and M. Zimmer, *AGIPD, a high dynamic range fast detector for the European XFEL*, (2014), [doi:10.1088/1748-0221/10/01/C01023]

[3] A.P. Mancuso, A. Aquila, G. Borchers, and K. Giewekemeyer, Scientific Instrument SPB (WP84); N. Reimers, Central Instrumentation Engineering (CIE), *Scientific Instrument Single Particles, Clusters, and Biomolecules (SPB)*, (2013) https://www.xfel.eu/sites/sites_custom/site_xfel/content/e35165/e46561/e46876/e46903/e46908/xfel_file46909/TR-2013-004_TDR_SPB_eng.pdf

[4] B. Henrich, J. Becker, R. Dinapoli, et al.: "The adaptive gain integrating pixel detector AGIPD a detector for the European XFEL", Nuclear Instruments and Methods in Physics Research Section A: Accelerators, Spectrometers, Detectors and Associated Equipment 633, Supplement 1, S11–S14 (2011) doi:10.1016/j.nima.2010.06.107

[5] https://in.xfel.eu/readthedocs/docs/detectordocumentation/en/latest/calibration/index.html

[6] https://journals.iucr.org/s/issues/2019/01/00/gb5080/index.html

[7] T. Tschentscher et al. Photon Beam Properties at the European XFEL. Euro- pean XFEL GmbH Technical Report TR-2011-006, 2012.

[8] H. Graafsma. Requirements for and Development of 2 Dimensional X-ray De- tectors for the European X-ray Free Electron Laser in Hamburg. Journal of Instrumentation, 4(12):P12011, 2009.